Vibrational Assignments for High Molecular Weight Linear Polyethylenimine (LPEI) Based on Monomeric and Tetrameric Model Compounds

Shawna S. York, Scott E. Boesch, Ralph A. Wheeler,* and Roger Frech*

Department of Chemistry and Biochemistry, University of Oklahoma, Norman, Oklahoma 73019

Received January 10, 2003; Revised Manuscript Received June 19, 2003

ABSTRACT: Polyethylenimine-based systems provide an interesting alternative to poly(ethylene oxide)-based systems for investigation of polymer electrolyte properties. Vibrational spectra may be used to infer conformations of polyethylenimine, but unambiguous assignments of IR and Raman bands must first be available. Hybrid Hartree−Fock/density functional methods were used to calculate the vibrational frequencies, modes, and infrared intensities for DMEDA (a monomeric model for LPEI) and a tetrameric model for LPEI. These results were then used to help assign the experimentally observed bands in the infrared and Raman spectra of LPEI.

Introduction

The potential importance of ionically conducting polymer systems as electrolytes in a variety of applications, especially rechargeable batteries, has stimulated intense interest in these systems.[1−6] Insight into the local structure and composition of the amorphous phase of polymer electrolytes is particularly important because this phase appears to provide the primary conductivity pathway.[7,8] Fundamental understanding of the nature of local structures and molecular-level interactions in polymer electrolytes has been aided by use of vibrational spectroscopy[7,9−17] and quantum mechanical calculations;[18,19] this work to date has focused extensively on systems based on poly(ethylene oxide) (PEO) and glymes (methyl capped, very short chain PEO oligomers). It is useful to complement this work by considering a polymer having a backbone structure similar to that of PEO, but with the oxygen replaced with another heteroatom. Linear polyethylenimine, or LPEI, is structurally analogous to PEO, with an N−H moiety in place of the oxygen atom (see Figure 1). LPEI also has the ability to dissolve a variety of salts to form polymer electrolytes. There have been several conductivity studies previously reported on LPEI-based polymer electrolytes with dissolved sodium triflate,[20] sodium iodide,[21] and various lithium salts.[22−24] However, vibrational spectroscopic studies of PEI-based electrolytes have been hindered because complete vibrational mode assignments for LPEI are not available in the literature.

Just as spectroscopic studies of glymes have been used to further the understanding of ethylene oxide-based systems, it is useful to consider small-molecule model compounds for ethylenimine systems. The simplest model compound for LPEI is *N*,*N*′-dimethylethylenediamine (DMEDA, Figure 1). The vibrational analyses of DMEDA and a longer, tetrameric analogue of LPEI (designated PEI-4, Figure 1) were undertaken in order to gain a better understanding of the vibrations of poly(ethylenimine) and polymer electrolytes based on a poly(ethylenimine) host. We have previously published mode assignments for DMEDA based on a comparison of experimental Raman and IR spectra with vibrational frequencies and intensities obtained using hybrid Hartree−Fock/density functional calculations.[25] In this work, the experimental and calculated frequencies of DMEDA are compared with the experimental frequencies of LPEI. In addition, calculations on PEI-4 have been done to model LPEI more closely. These comparisons of DMEDA and PEI-4 frequencies to the experimental vibrational spectra of LPEI have allowed us to make vibrational mode assignments for LPEI.

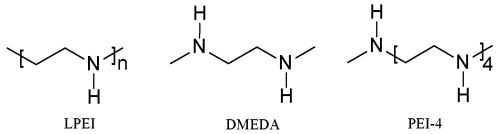

Figure 1. Linear polyethylenimine, *N*,*N*′-dimethylethlyenediamine, and the 4-monomer unit model compound PEI-4. The conformation of each C−N−C−C−N−C unit is not implied in the figures.

Experimental Section

LPEI (∼80 000 MW) was dried under vacuum at ∼75 °C for 48 h, dissolved in anhydrous methanol in a nitrogen-atmosphere glovebox (H_2O < 1 ppm), and stirred for 24 h. To obtain thin films of the samples, the polymer solutions were cast onto glass slides or Teflon sheets, and the methanol was allowed to evaporate at room temperature in the glovebox. The resulting films were dried under vacuum for 48 h at ∼45 °C.

Raman spectra were recorded using an ISA Jobin-Yvon T64000 Raman spectrometer. The 514 nm line of an argon laser was used as the exciting line at a power of 300 mW measured at the laser head. Raman spectra of the LPEI film were measured in a backscattering geometry through the 80× objective of a microscope. Raman spectra of the liquid DMEDA were measured in a sealed cuvette in conventional 90° geometry. Infrared spectra were recorded with a Bruker IFS66V FT-IR spectrometer over a range of 4000−400 cm^{-1} at a resolution of 1 cm^{-1}. The LPEI film was placed between AgBr plates in the evacuated sample chamber of the IR spectrometer at room temperature. Infrared spectra of liquid DMEDA were measured between ZnSe plates under a dry air purge. Overlapping bands in the FT-IR spectra were curve fit using Galactic Grams version 5.0.

Computations

The B3LYP hybrid Hartree−Fock/density functional method[26,27] and the 6-31G(d) split-valence plus polarization basis set[28] were used to perform complete geometry

10.1021/ma030016k CCC: $25.00
Published on Web 08/20/2003

Table 1. Experimental IR and Raman Frequencies (cm^{-1}) of LPEI, Calculated Frequencies (cm^{-1}) and Intensities (in Parentheses) of PEI-4, Experimental IR Frequencies (cm^{-1}) of DMEDA, Calculated Frequencies (cm^{-1}) and Intensities (in Parentheses) of DMEDA, and Mode Assignments for LPEI

LPEI IR	LPEI Raman	PEI-4 calcd	DMEDA[a] IR	DMEDA[a] calcd	LPEI mode assignments
	546	534 (0)			C−N−C bend
750 (sh)		791 (74)	736		N−H ⊥ bend
		806 (24)			
800	805	820 (91)	789	788 (84)	N−H ⊥ bend + CH_2 rock
855	853	826 (47)			CH_2 rock + N−H ⊥ bend
882		833 (71)	879	904 (15)	CH_2 rock + N−H ⊥ bend
931		934 (29)			N−H ⊥ bend + C−C stretch
		952 (7)			
962	962	958 (8)			C−C stretch + N−H ⊥ bend
1025		1021 (8)			CH_2 rock + N−H ⊥ bend
		1023 (7)			
1049	1046	1080 (82)			CH_2 twist + CH_2 wag
	1079	1095 (26)			C−N stretch
1107	1107	1107 (31)	1106	1115 (41)	C−N stretch
		1118 (60)	1122	1134 (23)	
1132	1134	1126 (25)			C−N stretch
		1129 (21)			
	1160	1150 (15)			CH_2 twist
1203		1204 (7)			CH_2 twist
1246	1245	1223 (42)	1251	1248 (3)	CH_2 twist
	1265	1252 (5)			CH_2 twist
1281	1290	1260 (12)			CH_2 twist
1330	1331	1323 (61)	1346	1342 (20)	CH_2 wag
1364	1367	1326 (27)	1361	1362 (3)	CH_2 wag
	1397	1346 (5)			CH_2 wag
1445		1442 (113)	1444	1444 (14)	N−H ∥ bend
	1451	1446 (126)			N−H ∥ bend
1471	1463	1469 (23)	1473	1476 (17)	N−H ∥ bend +CH_2 scissors
		1472 (23)			
1491		1484 (18)		1482 (14)	CH_2 sc+ NH ∥ bend
	2650−2926	2776−3001	2681−2967	2771−2958	C−H stretches
3220	3204	3334−3359	3280	3338	N−H stretch
3280	3290		3323	3363	

[a] Complete mode assignments and animated vibrations for DMEDA are available in ref 25.

optimizations and vibrational frequency calculations on PEI-4. The quantum chemistry program GAUSSIAN94[26] was used for all calculations. Berny's optimization algorithm[29] was used to perform full geometry optimizations in C_1 symmetry. Harmonic frequency calculations were performed at the optimized geometries without correcting for anharmonicity. It has become customary to scale calculated frequencies to facilitate comparisons with experiment; the multiplicative scaling factors of Scott and Radom[30] were used here. All frequencies less than 1000 cm^{-1} are multiplied by 1.0013, and all frequencies greater than 1000 cm^{-1} are multiplied by 0.9614. Vibrational mode assignments were performed by animating each mode using the program XMOL,[31] and the modes of PEI-4 were quantitatively compared to the modes of DMEDA by using vibrational projection analysis.[32,33]

Results and Discussion

A computational study of eight different conformations of DMEDA (TGT(0), TGT(1), TGT(2), GGG, GTG, TTG, TGG, TTT) as described in ref 25 determined that the lowest energy conformations are TGT.[25] Although a large number of possible conformations exist for PEI-4, the geometry optimization was begun from a TGT (trans−gauche−trans) conformation all along the chain; i.e., all C−C bonds are gauche. The PEI-4 geometry optimization results in C−N distances ranging from 1.458 to 1.464 Å and C−C distances of 1.528 Å. There are four intramolecular hydrogen-bonding interactions between adjacent N−H moieties with N−H···N hydrogen bond distances of 2.413−2.431 Å. These interactions

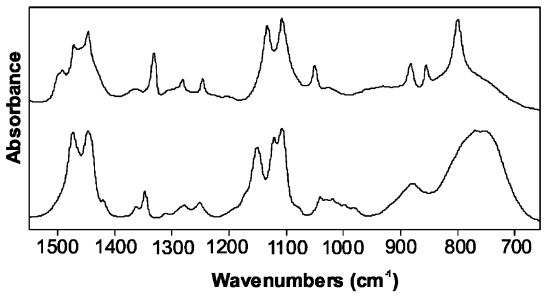

Figure 2. FT-IR spectra of DMEDA (bottom curve) and LPEI (top curve) from 675 to 1525 cm^{-1}.

are not traditional hydrogen bonds because conformational constraints prohibit a linear N−H···N geometry.[25]

Figure 2 displays the IR spectra of DMEDA and LPEI. A comparison of the data shows a good correlation between the bands of DMEDA and those of LPEI. Two comparisons were used in order to make the mode assignments for LPEI. Those LPEI bands that closely corresponded in both frequency and intensity to DMEDA bands were tentatively assigned to the same modes as in DMEDA.[25] Then the frequencies and absorbances were also compared to the scaled, calculated frequencies and calculated IR absorbances for the PEI-4 model. Mode assignments made for LPEI by comparison with DMEDA agreed well with those made by comparison with PEI-4. One notable difference is that several DMEDA modes with significant contributions from methyl wagging or twisting had much less of that contribution in PEI-4, and of course in high-MW LPEI

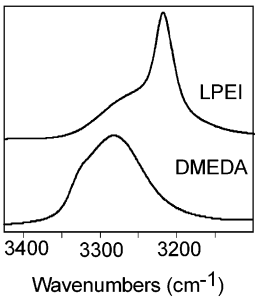

Figure 3. N−H stretching region in the IR spectra of LPEI and DMEDA.

the contribution of the methyl end groups to the vibrational modes was negligible.

Table 1 shows the experimental IR and Raman frequencies of LPEI, calculated frequencies and IR intensities of PEI-4, experimental IR and calculated frequencies and IR intensities of DMEDA, and mode assignments for LPEI. It should be noted that the experimental DMEDA spectra were taken of the liquid, which will exhibit a mixture of conformations. Two regions of the spectra are of particular interest in LPEI: from 700 to 1100 cm^{-1} and from 3000 to 3400 cm^{-1}. These regions may provide the best insights into the local structure of the polymer electrolyte based on the LPEI host. It has been reported that there are notable changes in the experimentally observed band frequencies and intensities in these two regions upon addition of lithium salts to DMEDA[34] and LPEI.[24] Further, the calculated frequencies and intensities of the modes from 700 to 1100 cm^{-1} in DMEDA have been shown to shift significantly when the conformation is changed.[25]

In the region from 700 to 1100 cm^{-1}, one can see in Figure 2 several differences between the IR spectra of LPEI and DMEDA. The vibrational modes in this region are primarily a mixture of N−H perpendicular bending (i.e., N−H bends that are perpendicular to the chain axis) and CH_2 rocking motions. The much sharper peaks in LPEI in this region are expected due to the highly crystalline nature of high-molecular-weight LPEI. The deviations in frequency between the high-MW LPEI and the calculated model compounds are not unexpected, due to the effect of interchain hydrogen bonding on the N−H bending frequencies in LPEI.[35]

In the region from 1100 to 1500 cm^{-1}, there are several types of modes: CN stretching from 1107 to 1134 cm^{-1}, CH_2 twisting from 1203 to 1290 cm^{-1}, CH_2 wagging from 1330 to 1397 cm^{-1}, and NH bending parallel to the chain axis and NH bending mixed with CH_2 scissors from 1445 to 1471 cm^{-1}. These spectral data clearly show that there is a very close correlation of the modes of DMEDA to those of LPEI, again illustrating that DMEDA is a good model for LPEI.

The N−H stretching modes are in the region from ∼3000 to 3400 cm^{-1}. In general, N−H stretching modes are very sensitive to hydrogen-bonding interactions; an increase in the strength of hydrogen bonding causes the frequencies to decrease.[36] It has been shown that disruption of hydrogen bonding in both DMEDA and LPEI systems (i.e., by dissolution of a salt) will shift these bands to significantly higher wavenumbers.[24,34] The much lower frequencies of the N−H stretches in LPEI than in DMEDA (seen in Figure 3) indicate a higher degree of hydrogen bonding in the former. The crystal structure of LPEI has been reported by Chatani et al. to consist of hydrogen-bonded double helices.[37] The sharp peak at 3220 cm^{-1} in LPEI originates in the crystalline phase of LPEI, while the shoulder at ∼3280 cm^{-1} originates in an amorphous phase of LPEI that appears to have weaker hydrogen-bonding interactions. In DMEDA, there is a broad peak around 3280 cm^{-1} and a shoulder around 3323 cm^{-1}. The higher frequencies of these modes indicate that the hydrogen-bonding interactions in DMEDA are less than in the crystalline phase of LPEI but comparable to the interactions in the amorphous phase of LPEI. The breadth of the DMEDA band also suggests a range of intermolecular hydrogen bond strengths.[25]

Summary

This work demonstrates that DMEDA and PEI-4 are good spectroscopic model compounds for LPEI. The vibrational mode assignments for high-molecular-weight LPEI have been made by comparing experimental IR and Raman spectra of LPEI to experimental IR spectra of DMEDA and calculated DMEDA and PEI-4 frequencies. It is shown that there is a good correlation of band frequencies in DMEDA and LPEI, except in the region from ∼700 to 900 cm^{-1}, where the more extensive hydrogen bonding in crystalline LPEI dominates the frequency patterns. In that region the detailed band structure spectroscopically observed in LPEI is not seen in DMEDA. However, the LPEI band structure is modeled well in this region by the PEI-4 calculations. In particular, the region from 750 to 900 cm^{-1} is important because these modes are sensitive to conformational changes in the backbone accompanying coordination of the nitrogen atom with a cation. Consequently, a careful study of these modes can provide useful insight into the nature of cation−polymer interactions in ethylenimine-based systems.

Acknowledgment. We are grateful to Albert Snow and Daniel Glatzhofer for synthesizing high-MW LPEI, NSF/NRAC for supercomputer time through Award MCA96-N019, the Oklahoma Supercomputing Center for Education and Research (OSCER), and NSF for funding DMR0072544.

References and Notes

(1) Bruce, P. G., Ed. *Solid State Electrochemistry*; University Press: Cambridge, 1995.
(2) MacGlashan, G. S.; Andreev, Y. G.; Bruce, P. G. *Nature (London)* **1999**, *398*, 792−794.
(3) Gray, F. M. *Solid Polymer Electrolytes: Fundamentals and Technological Applications*; VCH Publishers: New York, 1991.
(4) MacCallum, J. R., Vincent, C. A., Eds. *Polymer Electrolyte Reviews;* Elsevier Applied Science: New York, 1987; Vol. 1.
(5) MacCallum, J. R., Vincent, C. A., Eds. *Polymer Electrolyte Reviews;* Elsevier Applied Science: New York, 1989; Vol. 2.
(6) Ratner, M. A.; Shriver, D. F. *Chem. Rev.* **1988**, *88*, 109−124.
(7) Berthier, C.; Gorecki, W.; Minier, M.; Armand, M. B.; Chabagno, J. M.; Rigaud, P. *Solid State Ionics* **1983**, *11*, 91−95.
(8) Stainer, M.; Hardy, L. C.; Whitmore, D. H.; Shriver, D. F. *J. Electrochem. Soc.* **1984**, *131*, 784−790.
(9) Chintapalli, S.; Frech, R. *Electrochim. Acta* **1995**, *40*, 2093−2099.
(10) Ferry, A.; Orädd, G.; Jacobson, P. *J. Chem. Phys.* **1998**, *108*, 7426−7433.
(11) Frech, R.; Huang, W. *Solid State Ionics* **1994**, *72*, 103−107.
(12) Papke, B. L.; Ratner, M. A.; Shriver, D. F. *J. Electrochem. Soc.* **1982**, *129*, 1434−1438.
(13) Frech, R.; Huang, W. *Macromolecules* **1995**, *28*, 1246−1251.
(14) Huang, W.; Frech, R.; Johansson, P.; Lindgren, J. *Electrochim. Acta* **1995**, *40*, 2147−2151.

(15) Matsuura, H.; Fukuhara, K.; Tamaoki, H. *J. Mol. Struct.* **1987**, *156*, 293−301.
(16) Petersen, G.; Jacobsson, P.; Torell, L. M. *Electrochim. Acta* **1992**, *37*, 1495−1497.
(17) Rhodes, C. P.; Frech, R. *Macromolecules* **2001**, *34*, 2660−2666.
(18) Gejji, S. P.; Tegenfeldt, J.; Lindgren, J. *Chem. Phys. Lett.* **1994**, *226*, 427−432.
(19) Johansson, P.; Tegenfeldt, J.; Lindgren, J. *Polymer* **1999**, *40*, 4399−4406.
(20) Harris, C. S.; Shriver, D. F.; Ratner, M. A. *Macromolecules* **1986**, *20*, 1778−1781.
(21) Chiang, C. K.; Davis, G. T.; Harding, C. A.; Takashi, T. *Macromolecules* **1985**, *18*, 825−827.
(22) Chiang, C. K.; Davis, G. T.; Harding, C. A.; Takashi, T. *Solid State Ionics* **1986**, *18&19*, 300−305.
(23) Tanaka, R.; Fujita, T.; Nishibayashi, H.; Saito, S. *Solid State Ionics* **1993**, *60*, 119−123.
(24) York, S.; Frech, R.; Snow, A.; Glatzhofer, D. T. *Electrochim. Acta* **2001**, *46*, 1533−1537.
(25) Boesch, S. E.; York, S. S.; Frech, R.; Wheeler, R. A. *PhysChemComm* **2001**, *1*.
(26) Frisch, M. J.; Trucks, G. W.; Schlegel, H. B.; Gill, P. M. W.; Johnson, B. G.; Robb, M. A.; Cheeseman, J. R.; Keith, T.; Petersson, G. A.; Montgomery, J. A.; Raghavachari, K.; Al-Laham, M. A.; Zakrzewski, V. G.; Ortiz, J. V.; Foresman, J. B.; Cioslowski, J.; Stefanov, B. B.; Nanayakkara, A.; Challacombe, M.; Peng, C. Y.; Ayala, P. Y.; Chen, W.; Wong, M. W.; Andres, J. L.; Replogle, E. S.; Gomperts, R.; Martin, R. L.; Fox, D. J.; Binkley, J. S.; Defrees, D. J.; Baker, J.; Stewart, J. P.; Head-Gordon, M.; Gonzalez, C.; Pople, J. A. *GAUSSIAN94*; Gaussian, Inc.: Pittsburgh, PA, 1995.
(27) Stephens, P. J.; Devlin, F. J.; Chabalowski, C. F.; Frisch, M. *J. Phys. Chem.* **1994**, *98*, 11623−11627.
(28) Hehre, W. J.; Radom, L.; Schleyer, P. v. R.; Pople, J. A. *Ab Initio Molecular Orbital Theory*; John Wiley & Sons: New York, 1986.
(29) Schlegel, H. B. *J. Comput. Chem.* **1986**, *3*, 214−218.
(30) Scott, A. P.; Radom, L. *J. Phys. Chem.* **1996**, *100*, 16502−16513.
(31) Wasikowski, C.; Klemm, S.; Research Equipment, Inc., d.b.a. Minnesota Supercomputer Center, Inc., 1993.
(32) Grafton, A. K.; Wheeler, R. A. *Comput. Phys. Commun.* **1998**, *113*, 78−84.
(33) Grafton, A. K.; Wheeler, R. A. *J. Comput. Chem.* **1998**, *19*, 1663−1674.
(34) York, S. S.; Boesch, S. E.; Wheeler, R. A.; Frech, R. *PhysChemComm* **2002**, *5*, 99−111.
(35) Pimentel, G. C.; McClellan, A. L. *The Hydrogen Bond*; W.H Freeman and Co.: Berkeley, CA, 1960.
(36) Krueger, P. J. *Can. J. Chem.* **1967**, *45*, 2143−2149.
(37) Chatani, Y.; Kobatake, T.; Tadokoro, H.; Tanaka, Y. *Macromolecules* **1982**, *15*, 170−176.

MA030016K